Optimised Operation of an Off-grid Hybrid Wind-Diesel-Battery System using Genetic Algorithm

Optimised Operation of an Off-grid Hybrid Wind-Diesel-Battery System using Genetic Algorithm

Leong Kit Gan, Jonathan K.H. Shek, Markus A. Mueller*

Institute for Energy Systems, School of Engineering, The University of Edinburgh, The King's Buildings, Mayfield Road, Edinburgh EH9 3DW, UK

Abstract

In an off-grid hybrid wind-diesel-battery system, the diesel generator is often not utilised efficiently, therefore compromising its lifetime. In particular, the general rule of thumb of running the diesel generator at more than 40% of its rated capacity is often unmet. This is due to the variation in power demand and wind speed which needs to be supplied by the diesel generator. In addition, the frequent start-stop of the diesel generator leads to additional mechanical wear and fuel wastage. This research paper proposes a novel control algorithm which optimises the operation of a diesel generator, using genetic algorithm. With a given day-ahead forecast of local renewable energy resource and load demand, it is possible to optimise the operation of a diesel generator, subjected to other pre-defined constraints. Thus, the utilisation of the renewable energy sources to supply electricity can be maximised. Usually, the optimisation studies of a hybrid system are being conducted through simple analytical modelling, coupled with a selected optimisation algorithm to seek the optimised solution. The obtained solution is not verified using a more realistic system model, for instance the physical modelling approach. This often led to the question of the applicability of such optimised operation being used in reality. In order to take a step further, model-based design using Simulink is employed in this research to perform a comparison through a physical modelling approach. The Simulink model has the capability to incorporate the electrical and mechanical (Simscape) physical characteristics into the simulation, which are often neglected by other authors when performing such study. Therefore, hybrid system simulation models are built according to the system proposed in the work. Finally, sensitivity analyses are performed as a mean of testing the designed hybrid system's robustness against wind and load forecast errors.

Keywords: hybrid wind-diesel-battery system, off-grid, optimisation, isolated, genetic algorithm, renewable energy, modelling

*Corresponding author. Tel.: +44 (0)131 650 5629

E-mail address: leong.kit.gan@gmail.com (L.K.Gan)

1. Introduction

The concept of off-grid hybrid renewable energy systems are known as an attractive and sustainable solution for supplying clean electricity to autonomous consumers. Typically, this applies to communities that are located in remote or islanded areas where there is no connection to the main grid infrastructure and it is not cost-effective to extend the grid facilities to these regions. In addition, the use of diesel generators for electricity supply in these remote locations are proven to be high cost due to the difficult terrain which translates into high fuel transportation costs [1]. In addition, the carbon footprint of energy is also proven to be higher for the case of diesel-only solution [2]. A techno-economic study based on the rural areas in Sub-Saharan Africa has shown that the levelised cost of electricity (LCOE) of an optimised hybrid renewable energy system is lower than the LCOE obtained with standalone diesel generators [3]. The use of renewable energy sources coupled with the diesel generator allows for the cost of diesel fuel to be offset. However, to date, a common design standard for an off-grid system has yet to be found and the challenge in power dispatch strategy still exist while attempting to optimise the operation of an off-grid hybrid system. Moreover, the challenges increase disproportionately when multiple assets are combined. It is well-known that a diesel generator is recommended to operate at 40% of its rated capacity or higher to prolong diesel engine lifetime [4]. In addition, the continuous shifting of diesel engine between different operating states could possibly shorten its lifetime [5]. It is acknowledged that the user load profile is not constant throughout the day and it is often well below the suggested part-load diesel capacity. Furthermore, the situation becomes worse when the variability of the renewable energy sources is not taken into consideration while operating the hybrid system. The diesel generator's part loading problem can be alternatively mitigated by using a variable-speed diesel generator which was proposed in [6]. A comparison of the fuel consumption power curve between a fixed-speed and a variable-speed diesel generator has been carried out in [6]. The difference in fuel consumption between the two diesel generator types is small in the lower power ranges and non-existent above 65 kW [6]. One should evaluate the loading profile carefully as to whether or not the installed variable-speed diesel generator unit is economical as it utilises power electronics and permanent magnet generator which dramatically increases the control requirements, complexity and therefore the overall cost. In this work, the fixed-speed diesel generator is given attention to mitigate the part load.

The inclusion of batteries in a hybrid wind-diesel system allows a fixed-speed diesel generator to run at full load regardless of the load demand level at any particular time. In this case, the batteries are regarded by the diesel generator as an additional load in order to increase the power output closer to its rate capacity. In windy locations, the diesel generator is only switched-on whenever there is a lack of energy from the wind and battery

storage. An unknown matter in this case is the duration that the diesel generator should be operated. If a diesel generator runs for too long and charges the batteries to a high state-of-charge (SOC), the potentially available excess wind energy at a later time cannot be stored. Subsequently, excess energy is dissipated in a large dump load or wind power generation is curtailed. One way to help in matching the irregular pattern of the energy supplied from the wind to the load demand profile, is to install as much energy storage as possible. However, a hybrid system which has been designed in this manner will not be economical. This further emphasises the need to optimise the operation of a hybrid system, so that the energy storage system can be used efficiently to cope with drastic fluctuations in wind energy.

Tazvinga [7] has utilised model predictive control (MPC) technique to maximise the utilisation of renewable energy while minimising the operation cost and battery's charge-discharge cycles within a hybrid photovoltaic-wind-diesel-battery system. However, the diesel generator was scheduled to operate at part load condition within the considered time-frame. In a similar study, the MPC technique was applied in optimising the energy dispatch of a hybrid photovoltaic-diesel-battery system, with the aim of reducing the diesel generator use [8]. Nevertheless, frequent diesel generator power output variations were observed from the simulated results. As shown from the case study in Dhahran (Saudi Arabia), the diesel generator fuel consumption within a hybrid system is inversely proportional to the installed battery capacity [9]. Authors in [10] have proposed a stochastic dynamic multi-stage model to optimise the diesel dispatch operation of hybrid wind-diesel-battery systems. The proposed diesel dispatch strategy was compared against the load following and full-power strategies in [11]. In order to reduce the computational burden while seeking the optimal solution of the complex model, hourly time-steps were considered. Hence, the short-term peaks in the load demand were not considered. In literature [12], an optimised hybrid system which integrates demand response schemes and day-ahead forecasting of renewable energy resources and load demand was studied. However, it is noticed that the diesel generator was frequently changing its output power throughout the day. The optimisation strategy was carried out over a moving time-horizon in order to determine the optimal power references for various energy generation sub-systems. From the hybrid system sizing point of view, the authors in [13] have utilised Genetic Algorithm (GA) to optimise the PV tilt and surface azimuth angles angle by maximising annual energy production and other hybrid system components. The optimal system was designed for remote communities in Palestine with the cost of global warming emissions being taken into consideration. An improved GA was proposed in literature [14] for the use of hybrid system power generation. Its performance was compared against the standard GA in terms of convergence speed through the formulated scenario simulations. Besides satisfying electricity demand, a hybrid

system model which also provides water supply and hydrogen for automotive use is studied in literature [15]. A constrained optimal real-time operational management was presented for the case of hybrid system which integrates wind turbines, electrolyser, hydroelectric plant, pumping stations and fuel cell [15].

Despite the considerable work being carried out by the above-mentioned studies, the authors optimised their hybrid system's operation using only mathematical approach. The main drawback of this approach is the lack of mechanical and electrical considerations which take place in the real world, in particular, the physical dynamics of the system. The electrical transients which typically occur in the timescale of less than one second were not considered. In addition, most of the mathematical optimisations are performed in an hourly discretised manner, which further decrease the accuracy of the optimised results produced. For the case of larger power systems, sampling time with lower resolution is acceptable, because for instance, the total load demand and total wind power generation are aggregated from many households and wind turbines, respectively. In contrast, power fluctuations experienced by smaller power systems (in the scale of kW) can vary considerably [16]. It is known that if the day-ahead forecasted wind and load are available, the operation of the diesel generator can be optimised. A set of constraints such as the allowable range of battery SOC, the diesel generator capacity and the battery storage capacity are to be met within the optimisation problem. Other than integer programming optimisation techniques, which generate binary solutions, the solution produced by other optimisation algorithms can be of any value. However, integer programming has a restriction in which the objective function and the constraints are linear. Since it is desired to run the fixed-speed diesel generator at its rated power, the optimised solutions obtained from a non-integer programming technique need to be post-processed. This will be further described in the later sections. For the first time, this work proposes a methodology to optimise the operation of the diesel generator, by considering its efficiency and also reducing the start-stop cycles in order to safeguard its lifetime. Besides that, the author put emphasis on the electrical and mechanical considerations, through the utilisation of physical modelling after developing an optimised control solution mathematically.

The proposed simulation methodology is formulated in three steps, as presented in Fig. 1. First of all, the optimised solution is sought by optimising the diesel generator's operation using GA, based on the forecasted wind and load profiles which are discretised every 10 minutes. It is acknowledged that an accurate estimation of load demand and meteorological data present high cost and design complexity during its implementation stage [17]. There are several techniques to forecast short-term electricity load demand but mainly they can be classified into statistical and artificial intelligence (AI) techniques [18]. A recent AI-based load forecasting which utilised extreme learning machine theory is presented and its performance was benchmarked against

traditional models such as neural networks and adaptive neuro fuzzy inference system [19]. One of the approaches to predict the very short term (10 minutes) wind speed is by using the k-nearest neighbour (k-NN) classification model. This model uses wind direction, air temperature, atmospheric pressure and relative humidity parameters to predict wind speed [20]. However, a recently developed long-term (24 hours) forecasting wind speed model is more suitable to be used as the wind forecast input for this research if one desires [21]. Once obtaining the mathematically optimised diesel generator power dispatch strategy, it is to be processed such that the diesel generator should operate at its rated power with pre-determined timing operation. The detailed post-processed strategy is explained in the Section 2.6. Finally, the post-processed diesel generator's turn-on and turn-off time, forecasted wind and forecasted load demand are being fed into the hybrid system model which was developed using Matlab/Simulink.

The simulation is run for twenty-four hours simulation time. It is uncommon to run sophisticated Simulink models with such a long simulation time due to the long central processing unit (CPU) computation time and the limitation of random access memory (RAM). It took approximately four days in real time to complete one simulation using a computer with an Intel Core i7 3.40 GHz processor, 32GB of RAM and 64-bit Windows operating system. Finally, sensitivity analyses were conducted to test the robustness of the obtained solution. The proposed methodology which thoroughly investigates an optimised hybrid system is novel and the details are to be discussed in the next sections.

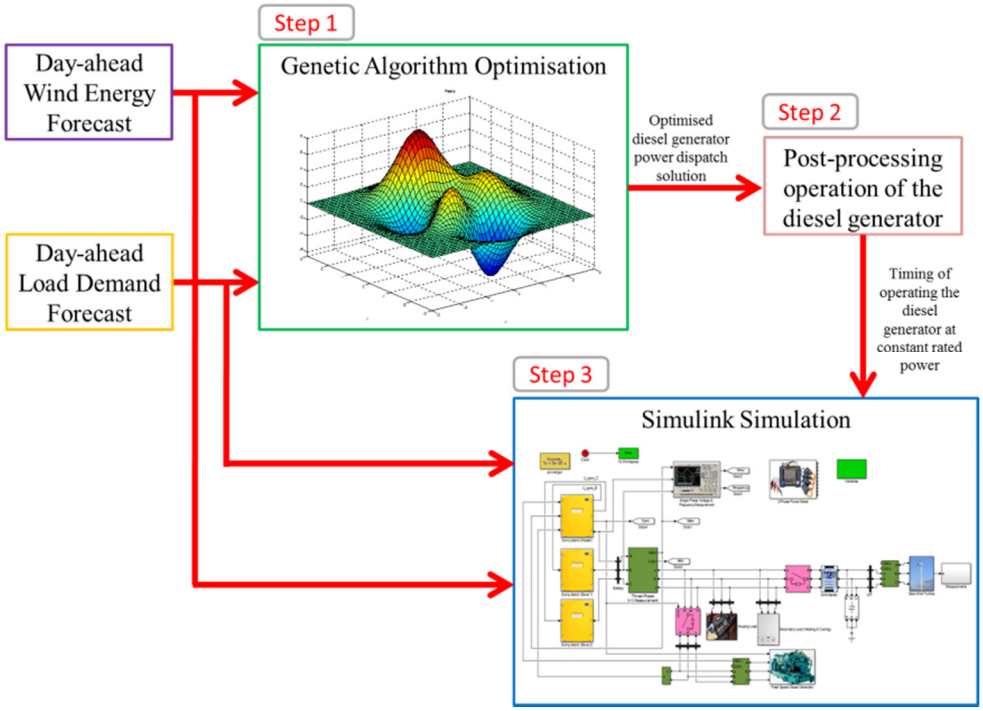

Fig. 1: Proposed simulation methodology

2. Modelling and Optimisation of Hybrid System Operation using Genetic Algorithm

This section describes the modelling and optimisation methodology for the operation of the hybrid system. The components of the hybrid system, described in a modular basis, are the battery grid-forming inverter, the fixed-speed wind turbine, the diesel generator, the wind profile and the load demand.

In literature, there are several optimisation algorithms that can be applied on optimising the performance of a hybrid system. GA which is classified as one of the evolutionary algorithms [22], is chosen in this work due to its capability of determining global optimum solutions over a series of iterations (generations) throughout the search space [23]. This is in contrast to local solutions determined by a continuous variable optimisation algorithm [24]. In addition, it is readily available in MATLAB's Global Optimization Toolbox and it conveniently enables the process of feeding the optimised results into Simulink software. The concept of GA was first introduced and developed in the mid-seventies. GA belongs to the class of stochastic search optimisation methods [25]. This simplified the programming process as they do not require the use of gradients of cost or constraint functions [24]. Biological evolution that is based on Darwin's theory of natural selection is comparable to the mechanics of GA, in which the language of microbiology and its application mimics genetic operations [25]. It can be used to efficiently optimise multi-dimensional, non-linear engineering problems.

The basic idea of a GA is to rather starting a single point (or guess) within the search space, it initialises with a population of guesses. Then, the GA generates a new set of designs (population) from the current set such that the average performance (fitness) of the design is improved. The process is continued until a stopping criterion is satisfied or the number of iterations (generations) exceeds a specified limit [23]. In this case, the inputs to the optimisation programme are wind and load data respectively. The programme minimises diesel fuel use subject to the following constraints:

- At any point in time, the total power generated by the wind turbine, battery storage and diesel generator must be greater than or equal to the load demand
- At any point in time, the energy stored in the batteries is the energy excess between the total power generation (from wind and diesel generator) and the load demand.
- At any point in time, the minimum SOC of the batteries should be greater than or equal to 20%.
- At any point in time, the power generated from the diesel generator should be less than or equal to its capacity

2.1 Battery Grid-forming Inverter Modelling

In this paper, the modelling of the hybrid system was developed in Matlab/Simulink, taking into account datasheets of commercially available components. The SMA Sunny Island (SI) bidirectional inverters [26] are utilised to form the isolated three-phase grid from the batteries. The AC and DC electrical specifications of the SI 8.0H are found in [26]. Fig. 2 shows the principle structure of the SI 4500 battery inverter [27] which is a predecessor of the SI 8.0H. In this work, the structure of Fig. 2 is adopted and it is assumed to be the same as the SI 8.0H, except that the nominal battery voltage is 48 V for SI 8.0H rather than 60 V. The battery is connected to a bidirectional Ćuk converter which boosts the DC voltage of the battery to a higher level [28]. The single phase AC voltage is obtained by inverting the DC voltage via the single phase inverter. From the literature [27], the topology used for the inverter is a bridge circuit. In addition, from the SI 8.0H's user manual [26], it is able to perform synchronisation with external power source. It can be concluded from the literatures that an SI inverter mainly consists of a bidirectional Ćuk converter, a bidirectional inverter and a synchronisation controller. The discussion on the synchronisation controller can be found in [29]. The detail modelling of the SI 8.0H was developed previously [30] and therefore, it will not be repeated here.

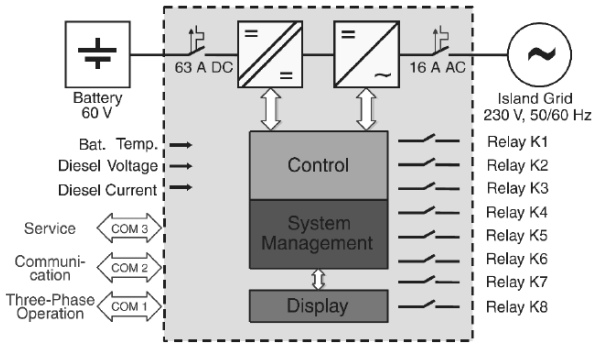

Fig. 2: Structure of the Sunny Island 4500 battery inverter [27]

2.2 Wind Turbine Modelling

A wind turbine converts the kinetic energy in wind into electrical power which can be used by consumers. Typically, wind turbines can be operated in fixed speed or variable speed. Fixed-speed wind turbine can only operate at a constant (or almost constant) for all wind speeds with predefined frequency power injection into the grid. In this work, the Gaia-Wind 133-11kW fixed-speed wind turbine is modelled. It consists of four main components: the blades, step-up gearbox, induction generator, and compensation capacitor for grid connection.

The theory of wind turbine aerodynamics is of importance for a designer to optimise power extraction from the wind. Its most fundamental formula is the mechanical power extraction of the rotor which is shown in equation (1) and the detail derivation of this formula can be found in [31].

$$P_{\mathrm{m}} = \frac{1}{2}.\rho.A_{\mathrm{R}}.V_{\mathrm{W}}^{3}.C_{\mathrm{P}}(\lambda,\beta) \quad (1)$$

where:

P_{m}: Rotor mechanical power (W)

ρ: Air density (kg/m^3)

$A_{\mathrm{R}} = \pi R^2$: Rotor disk plan area with radius R (m^2)

V_{w}: Wind speed (m/s)

C_{p}: Aerodynamic power coefficient of the turbine

The power coefficient, $C_{\mathrm{p}}(\lambda, \beta)$ is used to quantify the ratio of power extracted from the wind turbine to the theoretical power available in the wind. However, it does not represent a direct measure of the efficiency of the turbine. It is computed as a function of, tip speed ratio (TSR), λ which can be defined as equation (2) and pitch angle of the blades, β in degrees.

$$\lambda = \frac{R.\omega_{\mathrm{R}}}{V_{\mathrm{W}}} \quad (2)$$

where:

ω_{R} = Angular speed of the wind turbine rotor (rad/s)

In this work, the C_{p} for the Gaia's wind turbine is derived using experimental data provided in a report by TUV NEL [32]. Using this data, the λ values are derived accordingly. The C_{p}-λ curve is shown in Fig. 3.

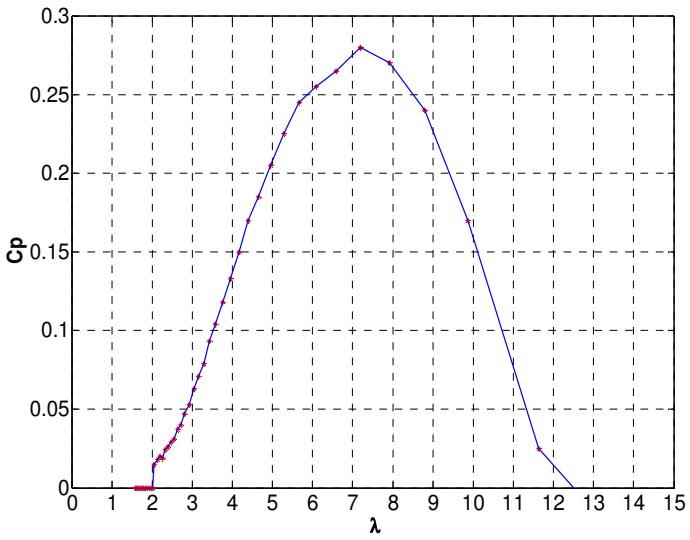

Fig. 3: C_{P}-λ curve for 133-11kW turbine

The step-up gearbox is represented by a simple mathematical function with mechanical torque at the low speed shaft and rotational speed of the generator as inputs. A 1:18 ratio gives the rotational speed at the rotor blades; the input power at the low speed shaft is then used to calculate the mechanical torque at the high speed shaft. The moment of inertia of the drive train is represented as a single element at the generator. Therefore, the moment of the inertia of the turbine rotor reflected back through the gearbox is required. This can be calculated using the following equation:

$$J_{\mathrm{r}} = \frac{J_1}{N^2} \tag{3}$$

The reflected moment of inertia J_{r} is the load inertia of the turbine rotor (J_1) divided by the square of the gear ratio (N). J_1 and N are given in a Gaia's report on aeroelastic loads [33].

2.3 Diesel Generator Modelling

A typical diesel generator structure is shown in Fig. 4 and it consists of an internal combustion (IC) engine and a wound-field synchronous generator coupled on the same shaft [34]. The wound-field generator requires an exciter and a voltage regulator to control the output AC voltage [34]. In this case, the brushless excitation system is provided by a small synchronous machine, thus avoiding the slip rings for providing DC power to the synchronous generator field. The AC voltage of the small synchronous machine is being rectified to DC using a rotating diode bridge that is mounted on the rotor shaft [34]. The governor is an electromechanical device used for automatically controlling the speed of an engine depending on load by adjusting the intake fuel. Generally, a governor can operate in two modes, i.e. the droop mode and the isochronous (constant speed) mode. The droop mode has a similar principle as discussed in the previous section on the droop control for SI inverters. In contrast, governors operating in isochronous mode will attempt to maintain the same frequency regardless of the load it is supplying up to the full rated capabilities of the diesel generator [35]. Typically, this mode of control is being used in an isolated system to maintain system frequency. However, in this work, the grid is formed by the SI inverters and therefore, the isochronous governor is not suitable to be used. Otherwise, the controllers would be in conflict, each trying to control system frequency to its own setting. Thus, the droop mode is applied on the diesel generator controller for parallel operation with the inverters.

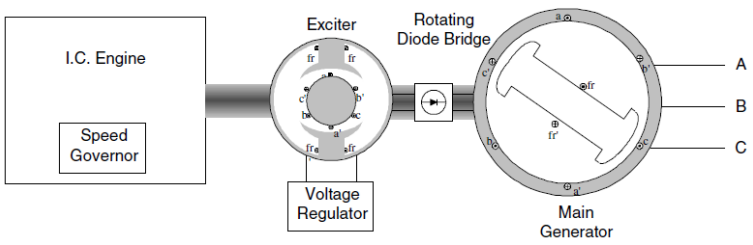

Fig. 4: Typical structure of diesel generator set [34]

Several control strategies of the diesel generator have been proposed in the past. In literature [36], the speed control of the diesel generator has adopted the fuzzy neural network (FNN) and the GA syncretic theory. The performance of such controller has been compared against the conventional PID control. In another study [37], the authors have applied MPC technique to estimate the plant model parameters, with the fuzzy logic supervisor measuring the performance criteria as input variables. More recently, the authors in [38] have developed an intelligent control solution which enhance the plug-and-play capability based on time-domain system identification experiments. However, a simple diesel generator control strategy is proposed in this work and its methodology is shown in Fig. 5. With the droop being set to a constant level, the diesel engine supplies a fixed amount of power to the generator regardless of the system frequency and the load demand at that particular time. The reference frequency for the governor is set to be higher than the grid frequency to ensure maximum power output is always achieved. This strategy also tries to reduce the number of start-stop sequences of the diesel generator, and at the same time running at its highest efficiency in order to reduce fuel consumption.

An emergency diesel generator which was modelled for nuclear power plant application [39] coupled with the above-mentioned droop control is implemented in this work. The diesel generator model is shown in Fig. 6, which consists of a governor, diesel engine, synchronous generator and dump load. The control system and the actuator are represented as a second order and third order [39] transfer functions, respectively. The speed-droop or regulation characteristic may be obtained by adding a steady-state feedback loop around the PI controller, as shown in Fig. 7. The droop value in this case is set to 0, which effectively representing a constant level. For the engine, it can be regarded as a pure time delay due to the time taken for fuel command to result in torque applied to the shaft [34]. The value of this time delay depends on the number of active cylinders in the engine and the shaft rotational speed [34]. For this work, a time delay of 0.024s is used [39]. The gains and time constants used in this model were adjusted empirically [39].

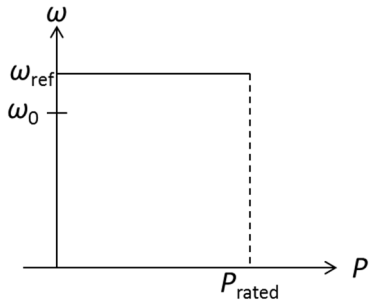

Fig. 5: Diesel generator droop characteristics which enable constant rated power output

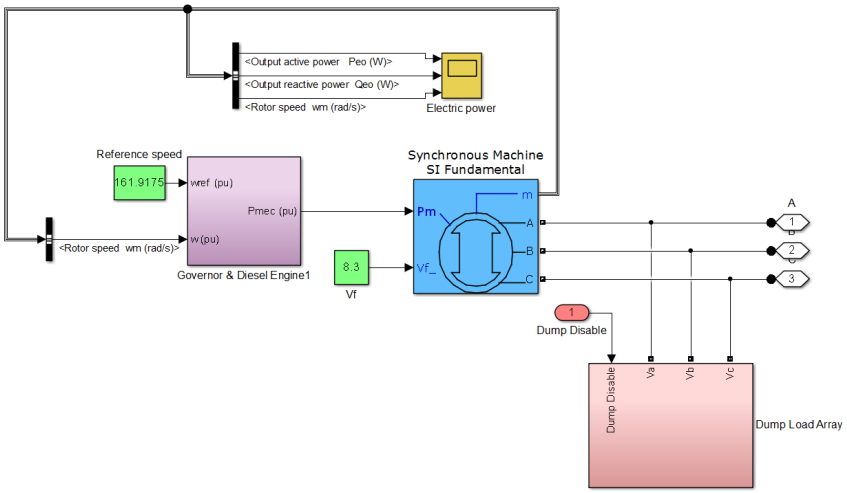

Fig. 6: Simulink model of diesel generator set

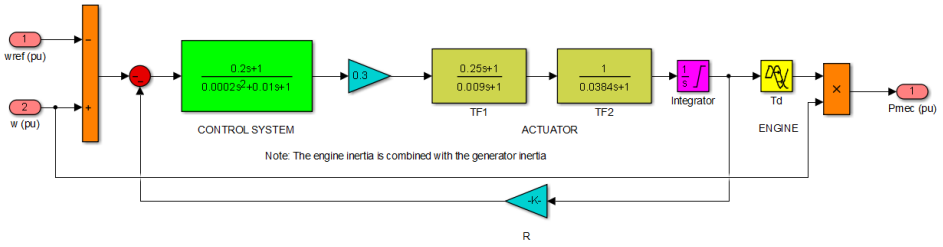

Fig. 7: Simulink model of diesel engine and governor

Dump loads are included at the output of the diesel generator to smoothen the transition of synchronising both diesel generator and the SI inverters. If the dump load is not included, the diesel generator voltage and current transients will be seen by the inverters during synchronisation. This might cause unnecessary voltage spikes due to the sudden increase in load. Note that the usage of dump loads in the system may incur additional installation and operation cost. Once the diesel generator is connected to the isolated grid, the dump loads are disconnected in steps. After all the dump loads are disconnected, the diesel generator operates at its rated condition, either supplying the load or charging the batteries if there is a surcharge of energy within the system.

2.4 Wind Energy Modelling

In this work, the historical wind speed data was taken from the Gaia-Wind Ltd's database (LeSENSE). The main objective of this paper is to demonstrate the decision of turning on the diesel generator optimally without charging the batteries unnecessarily as it is predicted that there is potential wind energy available at a later time. With this in mind, the author has selected a historical wind speed data which was measured in Aberdeen (Scotland) on 28/9/2011. Fig. 8 shows the wind profile using the wind speed data in which each data point is averaged over 10 minutes. It can be observed that the wind speed is moderately low from midnight until 8 a.m.

The highest wind speeds occur between mid-morning and mid-afternoon, reaching a peak of just over 9 m/s. In a non-optimise system, the diesel generator could turn on for a significant period of time in the morning and charge the batteries to a high SOC. Subsequently, the excess wind energy in the afternoon would be dissipated as waste energy as it cannot be stored in the batteries. The wind profile was then fed through the wind turbine power curve the power output from the wind turbine, as shown in the lower plot of Fig. 8. Note that power generation starts at approximately 3.5m/s wind speed.

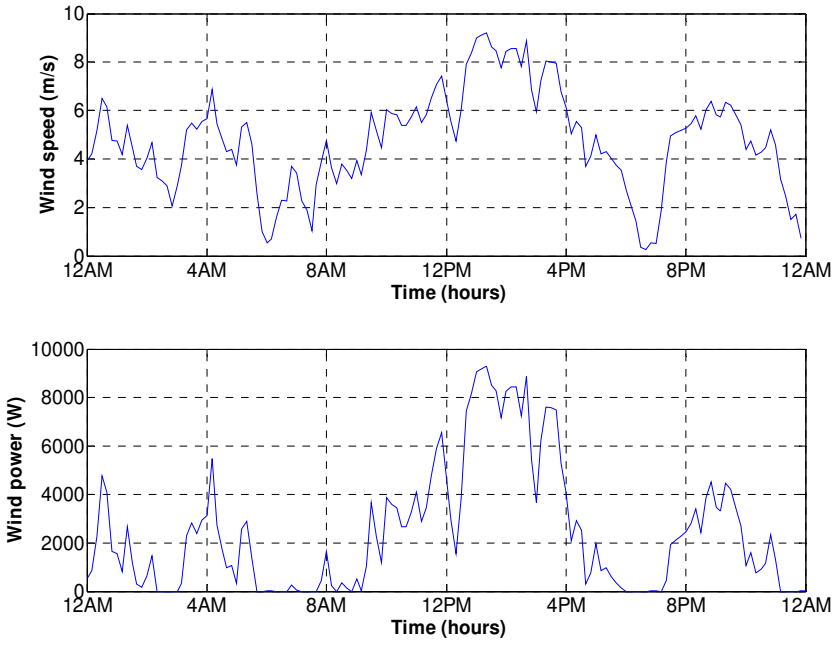

Fig. 8: Ten-minutes average wind speed and wind power in Aberdeen measured on 28/9/2011

It was stated before that if one hour sampling time resolution is adopted for the optimisation process, the probability of losing data (peaks and troughs) is high. In this work, the optimisation is carried out with a sampling time of 10 minutes. With this defined resolution, it is important to note that each data sampling point consists of only 1/6 of the hourly energy (kWh), i.e. kW10min. Therefore, care must be taken when working with this unusual energy convention. Fig. 9 shows the bar graph of the wind energy throughout the day. Each bar represents the absolute amount of energy generated from the wind turbine in 10-minute intervals.

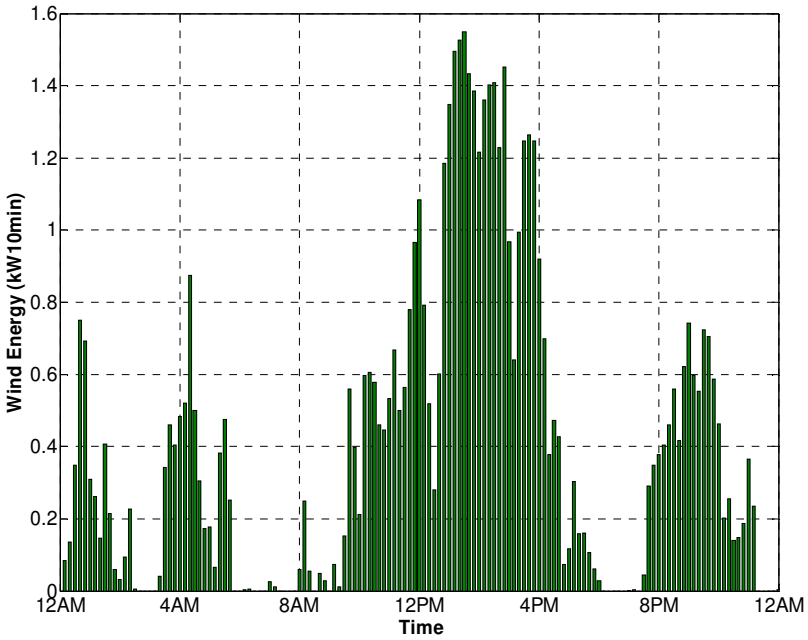

Fig. 9: Wind energy with a sampling time of 10 minutes (28/9/2011 in Aberdeen)

2.5 Load Modelling

A residential bottom-up electric load demand model which has taken into consideration of the relevant socioeconomic and demographic characteristics is reported in [40]. The "behavioural" and "engineering" probability functions were introduced in order to reproduce the psychological factors which affect the load demand. A similar 1-min resolution synthetic "bottom-up" energy demand model was developed in [41]. The model was quantitatively compared against the measured data sets which were recorded from 22 dwellings in the East Midlands, UK. The load model proposed in [42] has incorporated domestic hot water and space heating profiles, besides the common electric appliance load profile. The heating load profile has been produced with the integration of thermal resistant method and occupancy pattern control algorithm. Due to the measured load data is not freely available, this work has adopted a detailed bottom-up load model which was developed in [6] and it will be briefly described here for the sake of completeness. In addition, the load model in reference [6] was developed using Simulink software, which further reduces the complexity of utilising it in this research.

In the load model of this work, a defined time window has been associated for each action/event to take place (e.g. waking up, washing dishes, watching television and etc). A random number which was created for each activity, was then added onto the window starting time to determine exactly when the action will be started [6]. In addition, this model has assigned attributes to individuals so that they cannot perform irrational activity

such as vacuuming while using the computer and listening to the radio. Each electrical device consumes active power and reactive power. Since the power factor (PF) of a device can be related as:

$$\mathrm{PF} = \cos\theta = \frac{P}{S} \tag{4}$$

and the vector triangle of P, Q and S can be expressed as:

$$S = \sqrt{P^2 + Q^2} \tag{5}$$

The reactive power of a device is obtained as:

$$\mathrm{Q} = \sqrt{\left(\frac{P}{\cos\theta}\right)^2 - P^2} \tag{6}$$

Typically, a household contains several electrical devices which can be categorised as electronics and entertainment, lighting, motors and heating [6]. Electronic and entertainment devices such as televisions, personal computers, radios, game consoles generally contain switch mode power supplies (SMPS). The smaller power ratings SMPS (below 75W) do not require power factor corrections whereas devices above 75W are required by law to maintain a given power factor under regulation standard EN61000-3-2. Therefore, it can be concluded that the smaller SMPS loads have lower PF. Several lighting options for a typical household are the incandescent, compact fluorescent light, and fluorescent lamp. Small single phase motors (usually induction) which can be found in fridges, washing machines, dishwashers and other small pumps and fans throughout the property. Finally, the electrical devices for heating purposes consist of electric heaters, kettles, water heaters, microwave and irons. Table 1 tabulates the power factors being associated for various electrical devices modelled in this work. Their corresponding reactive power can be computed using equation (6).

Category	Electronics		Lighting			Motors	Heating	
Type	SMPS (< 75W)	SMPS (> 75W)	Incandescent	CFL	Fluorescent Lamp	1-phase Induction	Space / Water	Microwave / Iron
Power factor	0.63	0.98	0.99	0.95	0.9	0.83	0.99	0.83

Table 1: Electrical devices power factor [6]

Fig. 10 shows the overview of the load model which was implemented in Simulink. It consists of daily scheduling block, elapsed time activities block, and various electrical devices which consume different level of active and reactive powers based on their power factors and power ratings. It is important to emphasise that this model was built based on two full-time (9am to 6pm) working adults occupancy in mind, therefore no activities were taken place in the afternoon.

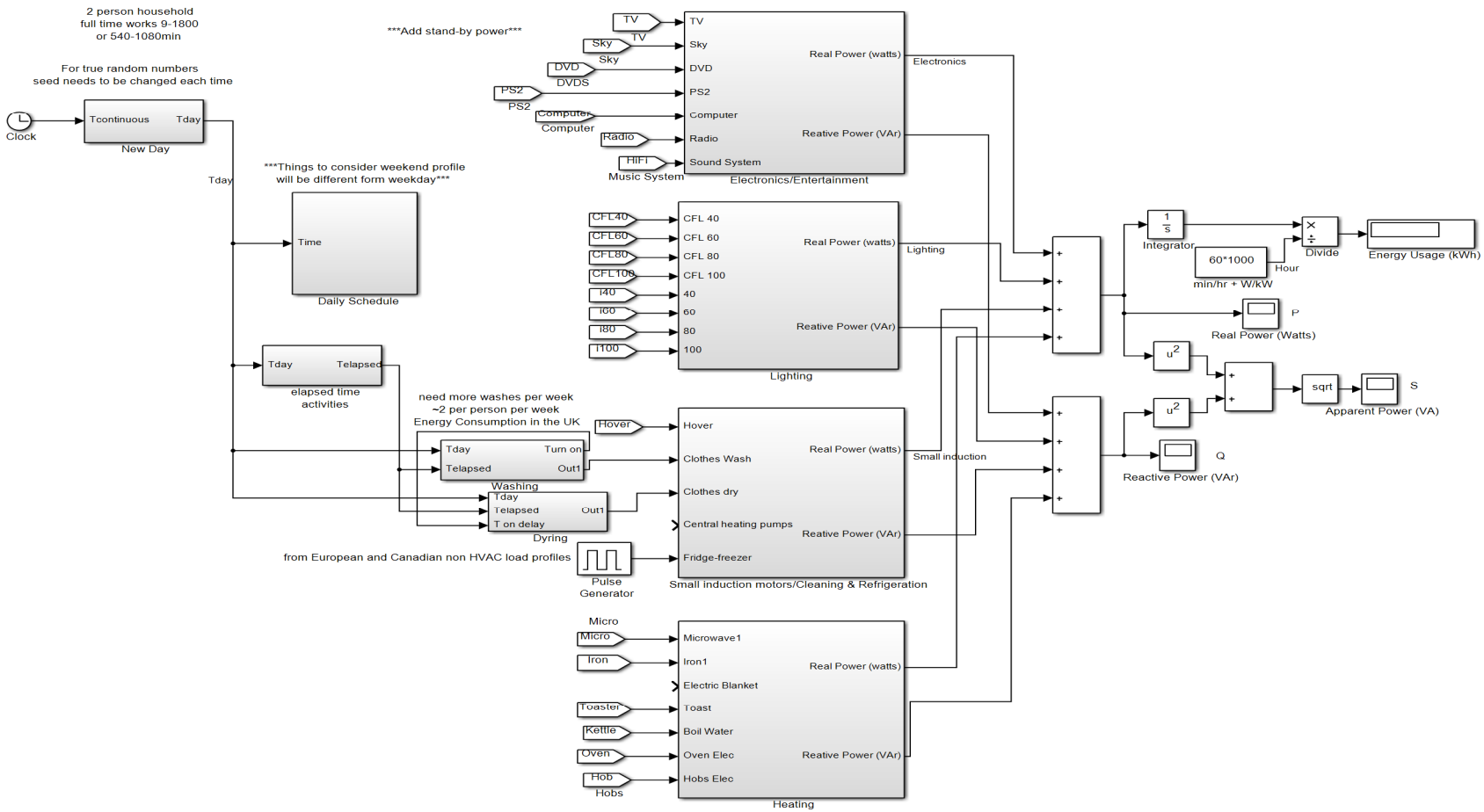

Fig. 10: Overview of load Simulink model [6]

The scheduling block controls the household member's waking up and sleeping time. This information is then used for the device usage and task execution in the household. In addition, the design of the building and layout of the devices in each room has been considered in the scheduling process. It means that links has been made between the electrical appliances and the rooms. For example, when the TV in the living room is switched-on during night time, the lights in the living room will be turned on and the lights in the kitchen will be off if no one is using any kitchen appliances. Furthermore, most of the electrical appliances usage is directly linked to the human attributes which consists of ears, eyes and hands. Some appliances such as the computer and game console require hands, eyes and sometimes ears. Other tasks are effectively obstructing the use of some human attributes [6]. For instance, vacuuming requires the use of hands and eyes but obstruct the use of ears for other activities. On the other hand, some devices can be used by multiple people at the same time for example watching TV, playing games and listening music together [6]. A single household load profile (Fig. 11) was generated by running the complete load model in Simulink. The resulted energy used per day was 18.69 kWh, which is close to UK's typical single household usage.

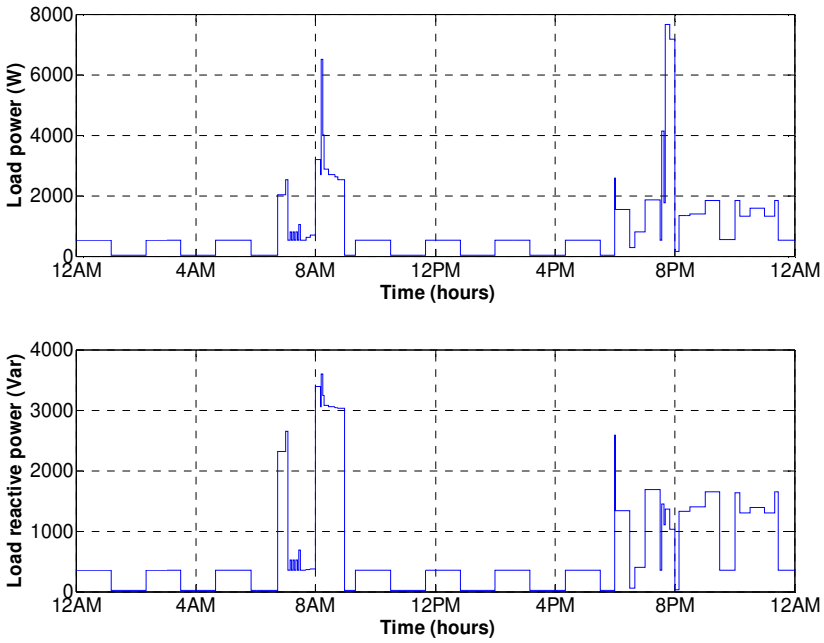

Fig. 11: Single household load profile (active and reactive power) [6]

A closer examination on the load profile shows that there are several distinct phases throughout the day. From midnight until about 7am, only the base load is noticed, which consists mainly the refrigeration compressor cycles and the standby loads. A pulsing sequence is observed from the refrigerator as the thermistor reads the temperature of the fridge and turn on the compressor when the upper pre-set temperature threshold is

met. The same principle applies for the turn-off sequence. The next phase occurs between 7am and 9am where people wake up, turn on the lights, make breakfast and get ready to work. The final phase is the post-work period which the peak load commonly occurs. Various domestic chores (washing, ironing, vacuuming and cooking for dinner) and enjoying in-house entertainments (TV, PC, radio and video games) took place during the night period. All in all, the resulting load profile is sufficiently realistic as the main objective of this work lies on the optimal operation of the hybrid system as a whole.

Keeping in mind that the optimisation procedure proposed here works with 10 minutes resolution, the load profile thus needs to be translated to the same convention as the wind energy described above. In addition, the active power demand of the system is only of interest in this case. Fig. 12 illustrates the load energy profile with 10 minutes sampling time, i.e. each bar consists of the amount of energy used by the consumer in 10 minutes. Comparing it to the upper figure of Fig. 11, it is noticed there is loss of data due to the lower sampling rate. The peak demand which was occurred just after 8am is not visible in Fig. 12. In addition, the duration of the peak demand which happened just before 8pm was shortened as a result of the down-sampling process took place. A higher sampling rate is possible to capture these peaks, however this comes with the compromise of longer computation time during the optimisation process. A higher sampling rate optimisation has been attempted in this work and it resulted with an insignificant amount of accuracy and it is thus not "economical" in this case.

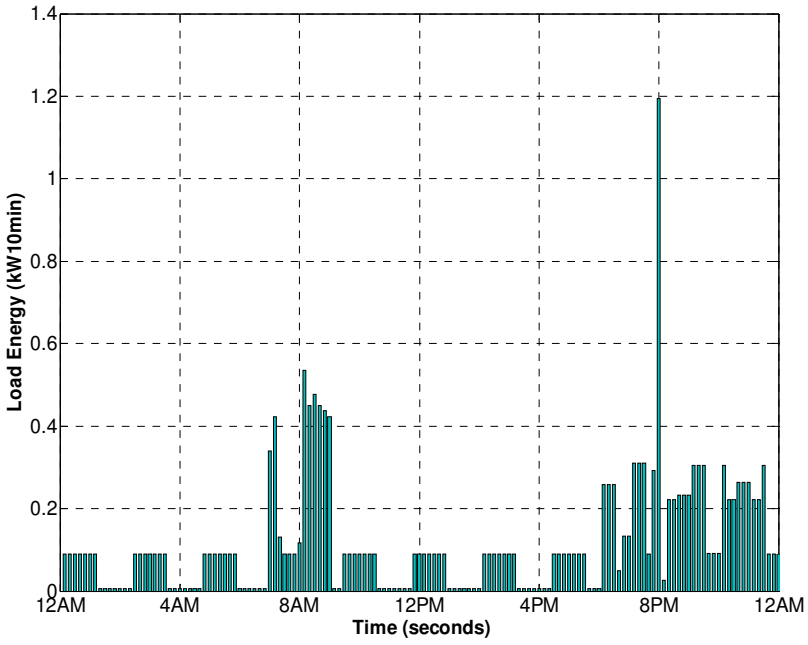

Fig. 12: Load energy profile with a sampling of 10 minutes

2.6 Optimisation Results

With the wind and load data being made available, optimisation on diesel generator operation can then be performed. From the long term cost analysis in [43], a hybrid system which consists of a Gaia Wind Turbine (11 kW power rating) is more economical to supply electricity to about three to four households. In other words, the cost of energy will increase if too little or too much load being supplied [43]. In this case, three households were considered as it achieved the lowest cost of energy scenario. The storage size in this case was set to 45 kWh. The specifications/conditions for hybrid system to be optimised is summarised in Table 2.

Specifications/Constraints	*Values*
Gaia wind turbine power rating	11 kW
Number of households	3
Batteries capacity	45 kWh
Initial battery SOC	20%
Minimum SOC at all time	20%
Diesel generator capacity	8 kW

Table 2: Specifications for optimised hybrid system

The objective of this optimisation is to minimise the diesel fuel use, subject to various pre-defined constraints. The diesel generator fuel consumption curve as a function of power output is illustrated in Fig. 13 and the corresponding fitness function (objective function) is given as equation (7) [43]:

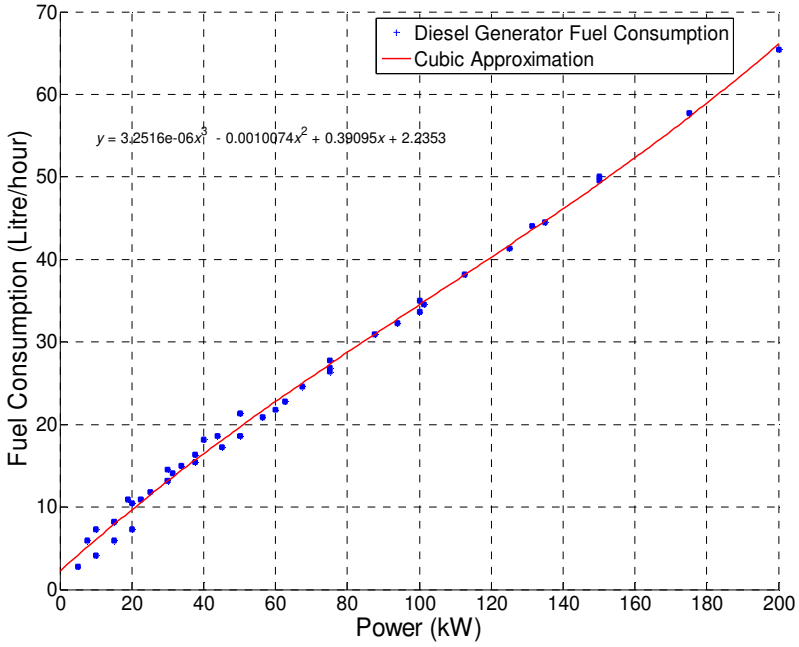

Fig. 13: Cubic fit of diesel generator fuel consumption [43]

$$F = 3.2516e^{-6}P^3 - 0.0010074P^2 + 0.39095P + 2.2353 \quad (7)$$

The optimisation results are shown in Fig. 14. The data points with reference to the y-axis on the left represent the energy production from wind turbine and diesel generator, and the load energy dissipation in 10 minutes intervals. The right axis shows the absolute energy level of the batteries in 10 minutes intervals. The batteries began with a SOC of 20% which corresponds to 9 kWh. The GA optimisation was run for 500 generations (iterations). The optimised diesel generator energy output can be seen from Fig. 14 (blue line).

At around 8am, the wind energy and the battery SOC were low while the load demand was quite high. In order to satisfy the minimal battery SOC constraint, the diesel generator started its operation to maintain the energy level of the batteries at approximately 20%. However, the diesel generator did not operate for longer than it was needed because of the significant amount of wind energy predicted to be available in the afternoon. It is noticed that the batteries started to charge at around 10am when the wind speed increased. Thereafter, the load in the evening was supplied from the charged batteries and the wind. Note that the overall utilisation of wind energy for the operation is high, which further justifies that the designed system is more sustainable and environmental friendly. Despite having the desire of operating the diesel generator at its power rating, it is not possible to be computed directly from the adopted optimisation algorithm. This is because a decision variable was being utilised in the optimisation model. A decision variable is a quantity that the solver computes and user has no control over it.

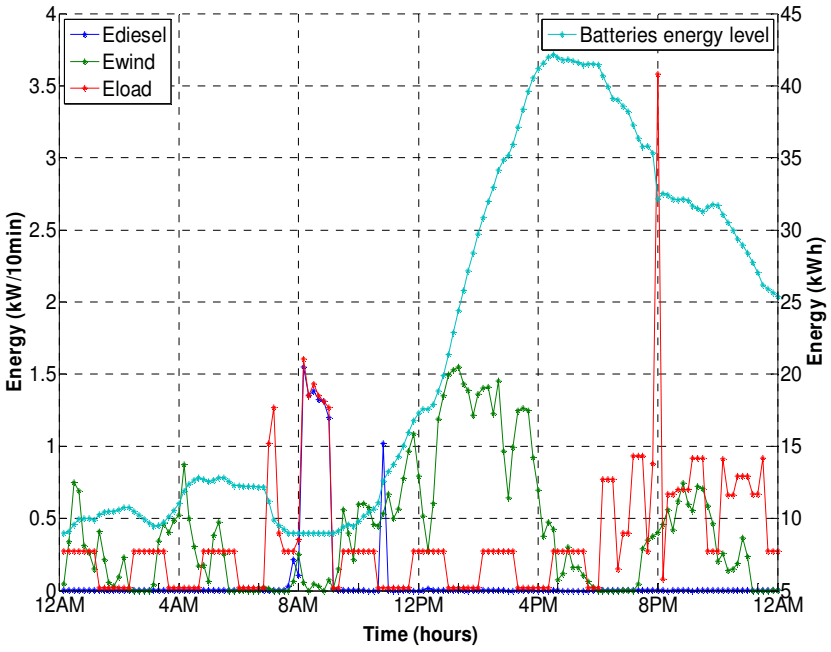

Fig. 14: *Left axis*: energy generation from the wind turbine, diesel generator and energy consumption from the load. *Right axis*: batteries absolute energy level

The diesel generator's power dispatch control is more complex if they were to operate according to the pattern as shown in Fig. 14. A sophisticated control system would need to be implemented to allow fast power output variation of the diesel generator. In addition, the lifetime of the diesel engine might be compromised if a complicated control system is employed as it will trigger the diesel generator to operate at part load condition on many occasions. Therefore, this work has proposed a method to process the diesel generator energy generation values obtained from the optimisation before putting into good use. This reduces the complexity of the control system within the diesel generator as it is programmed to operate at its rated capacity whenever it is switched-on.

A time window of two hours was formed, resulting in twelve windows throughout the day. Each window consists of 12 data points due to the 10 minutes sampling time used here. The proposed windowing method on the diesel generator power output is illustrated in Fig. 15. The diesel generator energy output within a window was accumulated. If there were any energy generation within that particular time window, the diesel generator was operated for 10 minutes at its rated capacity. If the accumulated value was greater than the power rating of the diesel generator, it was set to continue its operation for the next 10 minutes. This process continues until the accumulated value was less than the total energy generated from the diesel generator at rated power. In this work, the diesel generator has a power rating of 8 kW, which is capable of generating 8 kWh of energy in one hour. The amount of energy generated in 10 minutes is thus 1.333 kWh (8 kWh divided by 6).

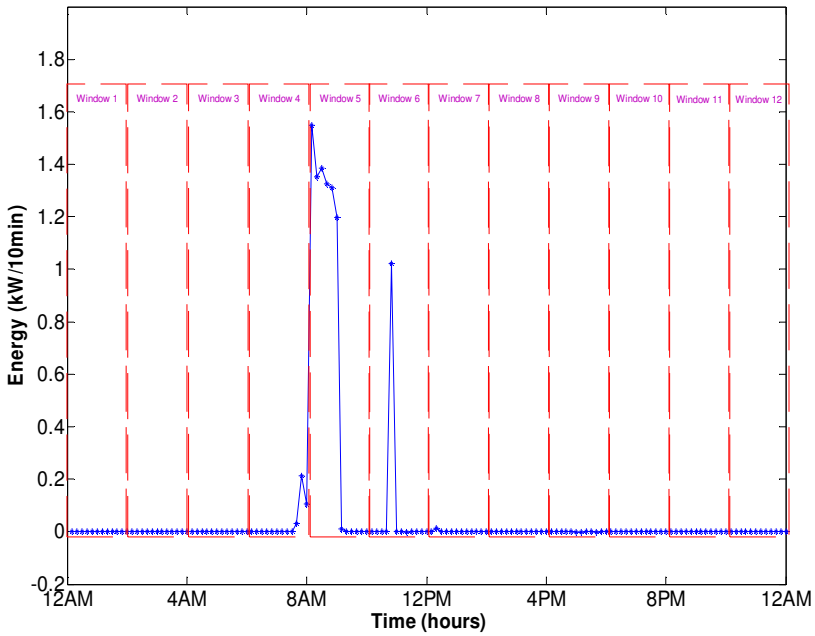

Fig. 15: Windowing of the diesel generator output

Fig. 16 shows the operation of the hybrid system after post-processing the diesel generator output. Notice that the diesel generator was operating at its power rating whenever it was turned on. As a result, the SOC profile within the day was also altered. As an example, considering the time frame within the Window 5 (8am to 10am) in Fig. 15, the accumulated diesel generator energy output was 6.58 kW10min. After performing the accumulation process as described above, the diesel generator operated for 50 minutes at its full capacity, generating in a total of 6.67 kW10min. Although this was slightly more than the optimised value (6.58 kW10min), the diesel generator was believed to be able to operate more efficiently (fuel efficient) and therefore, prolonging its lifetime. The corresponding altered charging profile of the batteries is shown in the right axis of Fig. 16. All in all, this strategy has reduced the frequency of on/off switching (which depends on the sampling time of the optimisation and the number of windows used in a day) and has prevented the diesel generator to operate at low load condition, which potentially jeopardised its lifetime. It is worth mentioning that the start-stop frequency and period of the diesel generator can be adjusted by changing the time windows in a day or using a diesel generator which has a different power rating.

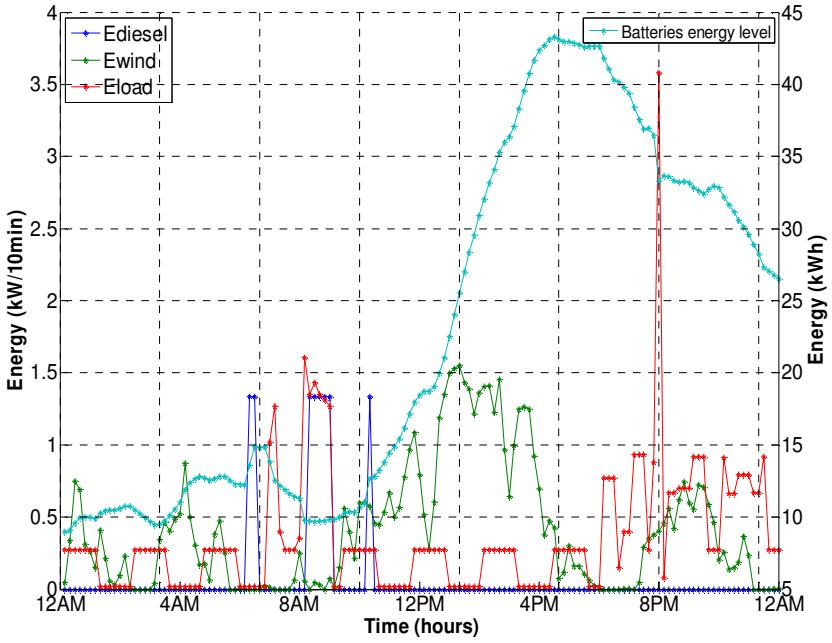

Fig. 16: *Left axis*: post-processed diesel generator energy output. *Right axis*: post-processed batteries absolute energy level

3. Simulation of an Optimised Hybrid Wind-Diesel-Battery System

After optimising the hybrid system operation mathematically, it is worth testing it in the Simulink to observe the dynamics and transients of the system. If this is not being conducted, more uncertainties regarding the applicability of the optimisation results in the real system exist. Ultimately, this step is performed to give more

confidence and it provides a better understanding of the results obtained from the mathematical models. Using the developed Simulink model, a simulation time of 86400 seconds (24 hours) was performed. In this work, the author has split up the simulation run time. The simulation state and the desired variables are saved after 3600 seconds (1 hour) simulation time. The variables were then cleared to free up some memory space for the next simulation run time. This can be repeated in order to extend the overall simulation time period. The sampling time of the simulation is 50 µs and the recorded data was decimated by a factor of 100. The Simulink model of the hybrid system which was used to study one day of operation is shown in Fig. 19.

The load model is being implemented with the three-phase dynamic load block which is available in SimPowerSystems (Simulink library). The active power and reactive power were controlled from the external input. With this approach, the load profiles of Fig. 11 are emulated. In order to achieve a more realistic simulation, the 10-minutes average wind speed (Fig. 9) was used in conjunction with the turbulent wind model which was previously developed in [44]. The turbulent wind model block diagram is shown in Fig. 17. The corresponding synthesised turbulent wind profile is shown in Fig. 18. Intuitively, the turbulence intensity is greater at a higher wind speed. This principle is well demonstrated in the turbulent wind profile below.

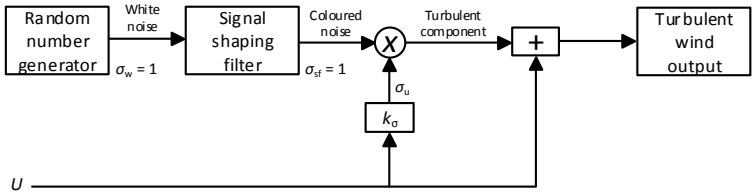

Fig. 17: Turbulent wind model block diagram [45]

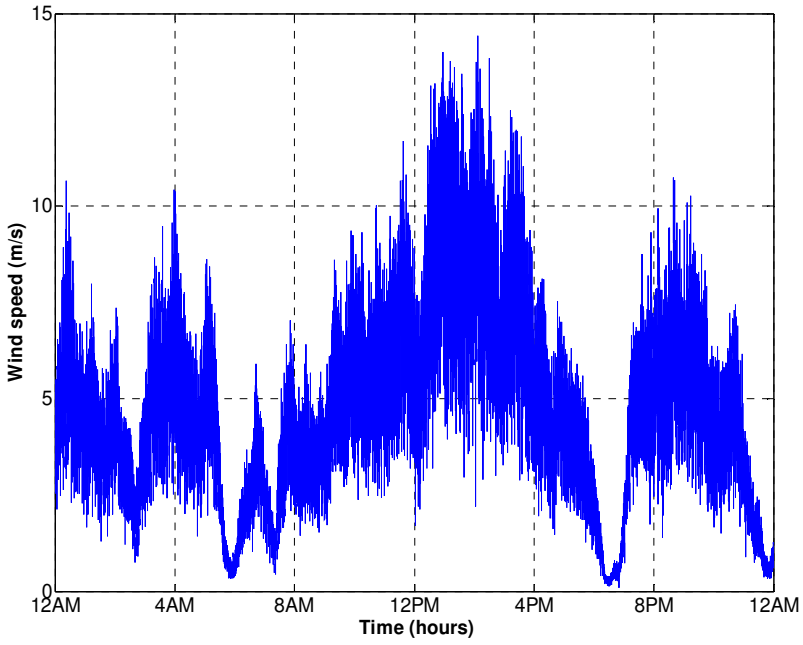

Fig. 18: One day's synthetically generated turbulent wind profile

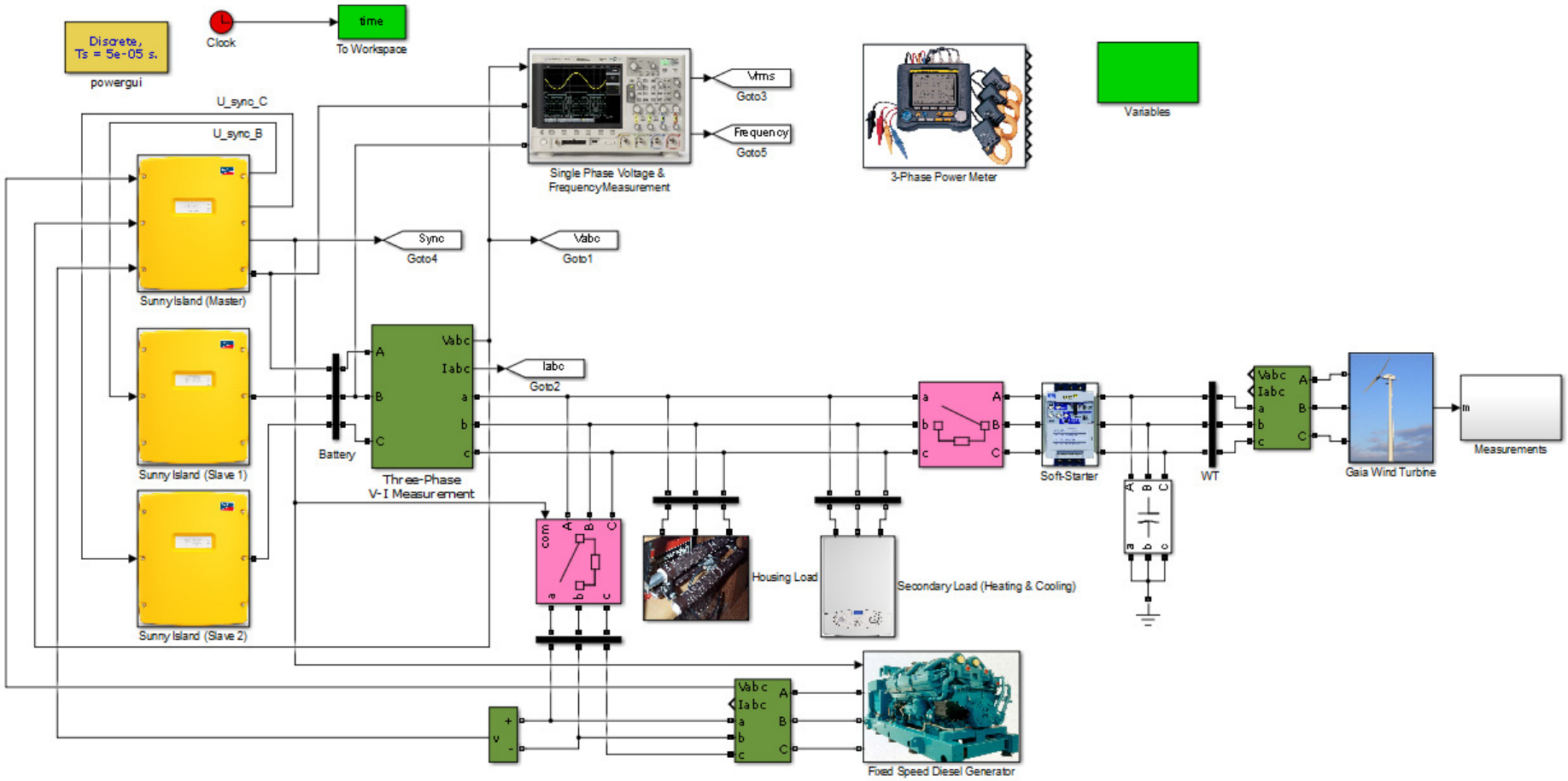

Fig. 19: Hybrid system Simulink model used to run for 24 hours simulation time

The start-stop cycle of the diesel generator is based on the post-processed profile. It generates 8 kW (rated power) whenever it is switched-on. A safety precaution which is used to prevent the batteries from over-discharged as a result of any unexpected events or errors in wind & load forecasts has also been implemented. In particular, the diesel generator is switched-on whenever the SOC is less than 15%. To prevent frequent start-stop cycles, a hysteresis control has been adopted. This means that the diesel generator will only switch off when the batteries SOC reaches 25%, as the system will collapse or become unstable if the SOC is too low.

Fig. 20 shows the system frequency and line voltage throughout the day. Note that the frequency spikes occurred during the synchronisation and connection between the isolated grid and the diesel generator. Once the diesel generator was connected to the system, the frequency rose due to the higher availability of active power within the system. The most apparent frequency drop occurred just before 8pm, which was due to the peak in demand. At this point in time, the SI inverters operated almost at their rated value (6kW per phase). Several voltage drops were quite apparent and they can be associated with the higher reactive power demand during those periods. In general, the frequency and voltage were within the statutory limits throughout the simulation.

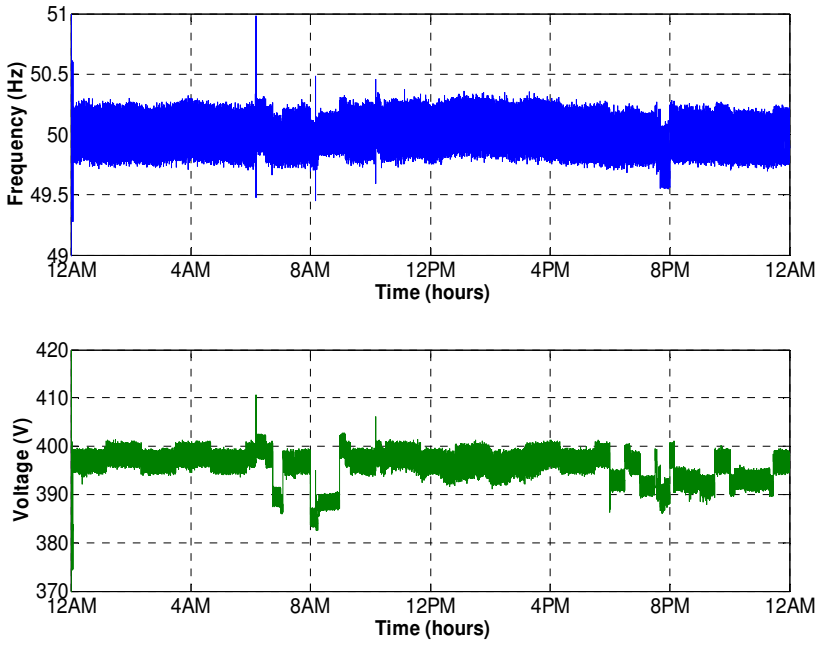

Fig. 20: System frequency and voltage over 24 hours period

Fig. 21 shows the comparison of battery SOC between the GA post-processed results (right axis of Fig. 16) and the Simulink results. It can be observed that the SOC trends for both correlate well. Some small discrepancies are mainly due to the power losses in the electronics components and machines, under-sampling of load profile in the GA optimisation, turbulent wind and electrical transients (delays from control systems).

Between about 1pm and 4pm, it is noticed that both of the SOC profiles began to diverge. This is due to the inability of the wind turbine to absorb the turbulent energy from the wind as a result of the disc-averaging effect possessed within a wind turbine. The high frequency components of the wind were filtered out mechanically. Another large diversion occurred at around 8pm, can be associated with the evening peak load. Inaccuracies are noticed as a result of the down-sampling of the load model when performing the GA optimisation. The peak load period in the Simulink simulation is slightly longer than that of the GA and hence, more energy is being discharged in the former case as observed in Fig. 21. Although the optimisation has a constraint to avoid the SOC of the batteries falling below 20%, a slight outrun is observed just after 8am. Thus, it is important to make sure that the SOC does not fall below the critical level by switching on the diesel generator. It is vital to perform further simulations in Simulink using the GA mathematical results in order to analyse the electrical characteristics and to identify the presence of any non-ideal or unusual operating behaviour. This increases confidence and understanding of the results generated by the GA.

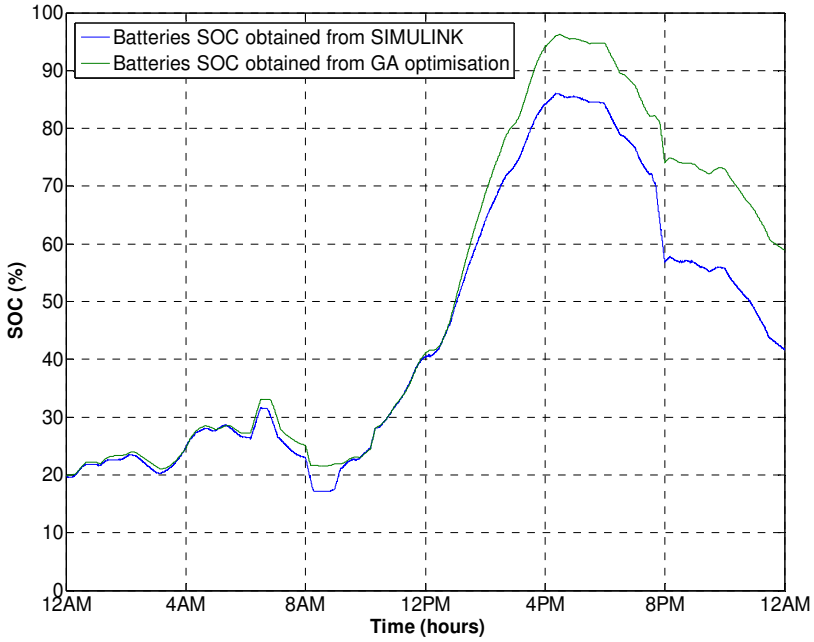

Fig. 21: Batteries SOC comparison between measurement from Simulink and computation from mathematical model

Fig. 22 shows the power flow from the wind turbine, the diesel generator and the battery storage via the SI inverters. The large fluctuations of the wind power can be linked to the turbulent effect of the wind. Despite having these variations, the hybrid system operated in a stable manner and having a good power quality which can be reflected from the system voltage and frequency (Fig. 20). It can be shown that the power generated from the wind turbine was limited to around 11 kW despite of the existence of high turbulent wind peaks (slightly less

than 15 m/s). This can be attributed to the drop in C_p when the TSR increased beyond 7. At a higher TSR, a high thrust force existed but lesser power being generated due to the smaller lift force. This is a common characteristic of a fixed-speed wind turbine [46]. The switching on/off cycle of the diesel generator was based on the optimised GA results. The diesel generator operated at its rated power whenever it was switched on. In this simulation, the safety precaution of the diesel generator was not being exploited because the SOC of the batteries never reach to a critical level of 15%. Finally, the power flow measured from the SI terminals is shown in the bottom plot of Fig. 22. This also corresponds to the charge and discharge cycle of the batteries. Throughout the day, the battery charging process took place more frequently, especially in the afternoon because it was quite a windy period. The SI inverters supplied power to the load whenever the wind power was not sufficient to meet the demand. It is worth mentioning that the batteries charge and discharge cycle graph can be used for battery lifetime analysis, however it is beyond the scope of this work to do so.

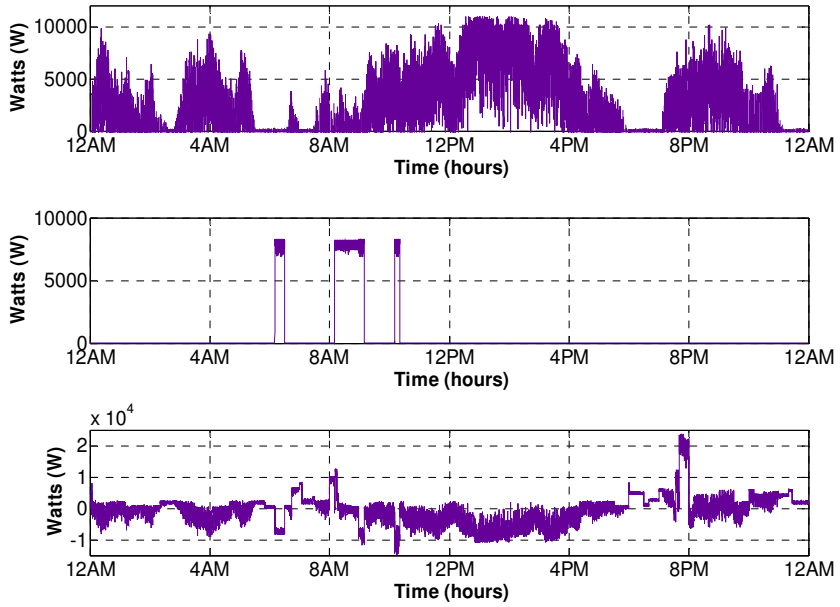

Fig. 22: *a)* Wind turbine power *b)* Diesel generator output power *c)* Charging and discharging power of the batteries

In summary to discussion above, the optimised hybrid system operation using GA performs well in the Simulink model. The verification from the Simulink model is a step forward to justify the feasibility of the proposed algorithm. However, it requires the fairly accurate prediction of wind and load profiles. The following section explores the non-ideal circumstances which are more likely to occur in real world such as under and over forecast of the wind speed and load demand. In particular, sensitivity analyses on the wind speed and on the load demand are performed.

4. Sensitivity Analysis of a Hybrid System with Optimised Operation

A sensitivity analysis can be defined as the study of how a system reacts to the uncertainty in its input. In this case, it is a vital step to be carried out after verifying that the hybrid system can be operated fairly well in an ideal situation, whereby the load and wind speed are forecasted perfectly. However, errors in load prediction and weather forecast can exist in reality. These are the input to the system and therefore, their sensitivity towards the system should be investigated. Typically, the errors of day-ahead load and wind speed forecast are analysed through statistical distributions [47]. In large power systems, these errors can have economic consequences as they can be a critical factor in ensuring near-optimal system operations. In off-grid systems, the fast-starting, more expensive diesel generator will be required to fulfil the load in an energy deficit situation. On the other hand, the renewable generations would need to be curtailed if there is energy excess which cannot be stored.

Load generally follows a familiar pattern, reaching its peak in the morning and evening. It was noticed from a study that the load forecasting error is accounted by numerous errors between 10% to 20% [47]. On the contrary, although wind speed displays some daily and seasonal characteristics, it follows less regular patterns compared to the load. The wind speed forecasting error is dependent on the length of the forecasting timescale [48]. A day-ahead wind speed forecast error has recorded values between 15% to 40%, depending on the methodology used [49]. For simplicity purposes, this paper proposes simple multiplication factors to be multiplied with the ideal load demand and wind speed forecast in order to emulate the forecast errors. Three different sensitivity analyses are proposed. In the first and second sensitivity analyses, constant multipliers were applied to the load profile and to the wind speed profile, respectively. Within these analyses, it is assumed that the three households turned on their loads at the same time. Finally, the second load sensitivity analysis is performed by having the load profile being aggregated with the assumption that all three households turned on their loads at a different times. The two proposed load sensitivity analyses were also conducted for comparison purposes and as a mean of testing the hybrid system's robustness against different types of load error forecasts.

A 3 kW and 5 kW secondary loads were included in the system in order to avoid the batteries being charged to 100% when the wind energy was high and the load demand was low. Each of them is connected to the isolated grid through a circuit breaker which is controlled using a simple hysteresis approach. The 3 kW load is switched-on when the batteries SOC was 85% and is switched-off when the SOC is equal to 80%. Similarly, the 5 kW load is switched-on and switched-off when batteries SOC reaches 95% and 90% respectively.

4.1 Load Sensitivity Analysis

In this study, the load profile of the three households was varied with a multiplication factor of ×0.8, ×1, ×1.2 and ×1.4, respectively. These proposed numbers were suggested in this work and they are reasonable based on the typical forecast errors found out in the past [47]. A multiplication factor of ×1 represents the ideal optimised operation from the GA, while the other multiplication factors represent under- or over-prediction of the load demand. The wind speed profile and the pre-set control of turning on the diesel generator (obtained from the results of GA optimisation) did not change for all cases. However, the diesel generator would be forced to run whenever the battery SOC dropped to less than 15%., as a result of safety pre-caution.

Table 3 tabulates the simulation results and Fig. 23 shows the SOC profiles for all the load multiplication factors. The system frequency and line-to-line voltage were averaged over 24-hour period. In all cases, they are within the statutory limits. As expected, the diesel generator turned on longer when the load multiplication was higher. It is noticed from Fig. 23 that the batteries SOC for the case of ×1.2 and ×1.4 became quite low just after 8am, and they dropped to about 10% despite the continuous operation of the diesel generator. The total diesel generator operation time was more than double with an additional load factor of ×0.4. However, the hybrid system was ensured to operate without failure. Therefore, the pre-included safety feature of the diesel generator increases the robustness of the hybrid system operation. A higher diesel generator power rating or a larger safety margin is required if the load of that particular household is expected to have a higher usage or larger variation. The latter can be done by setting the diesel generator to be switched-on when the batteries SOC drops to a level higher than 15%. An interesting observation from Fig. 23 is that the SOCs follow each other closely until the peak load which occurred at about 8pm. At that time, the diesel generator did not switch on at all because the energy stored in the batteries was sufficient to supply the load for the remaining time. Thus, the largest deviation of the SOC from the ideal case happened only when the peak load was occurred during high batteries SOC.

From Table 3, it can be observed that the 3 kW secondary load turn-on time reduces as the load multiplication factor increases. The batteries were prevented from being charged to 100% by switching on the secondary load. The 3 kW secondary load was switched-on about 3 times longer for the case of ×0.8 compared with multiplication factors of ×1 and ×1.2's scenarios. The batteries SOC of the former reached 85% for a relatively longer period and this can be attributed to the overall lower load demand. On all occasions, the 5 kW secondary load was not triggered to turn on because none of the batteries SOC reached 90%.

Load multiplication factor	*×0.8*	*×1*	*×1.2*	*×1.4*
Average frequency (Hertz)	50.01	50.01	50.01	50.01
Average line-to-line voltage (Volt)	396.17	395.75	395.32	394.96
Diesel generator turn-on time (minutes)	79.70	79.69	119.57	186.41
3 kW secondary load turn-on time (minutes)	156.50	54.08	49.58	0
5 kW secondary load turn-on time (minutes)	0	0	0	0

Table 3: Load sensitivity simulation results

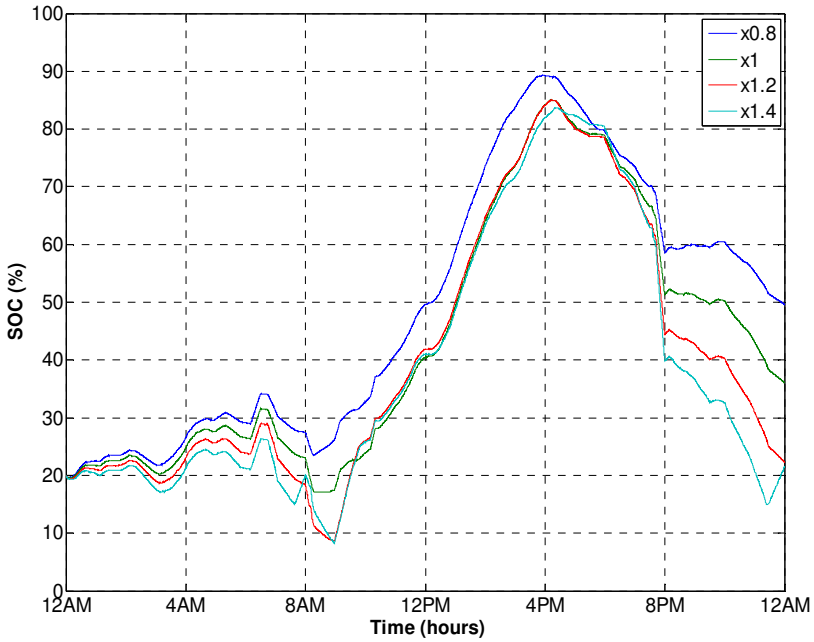

Fig. 23: SOC profiles for different load multiplication factors

4.2 Wind Energy Sensitivity Analysis

In this section, the wind energy sensitivity analysis was conducted by multiplying the wind speed profile (upper plot of Fig. 8) with a multiplication factor of ×0.8, ×1, ×1.2 and ×1.4 respectively. The load profile and the pre-set control of turning on the diesel generator (obtained from the results of GA optimisation) did not change for all cases. Table 4 and Fig. 24 demonstrate the simulation results of various wind speed multiplication factors. The average frequency and the line-to-line voltage over the day are within their statutory limits. A small increase in average system frequency was observed as the multiplication factor goes up. This can be explained by the frequency versus power droop characteristic exists within the modelled SI inverters, as shown in Fig. 25. A higher wind multiplication factor translates to a higher active power generation from the wind turbine. Hence, the frequency increased. However, the average line-to-line voltage was decreasing as the wind multiplication factor increases. This is due the fact that an induction generator consumes more reactive power when the active power generation increases. The diesel generator operated for an additional 2 hours and 20 minutes when the wind speed was reduced by a factor of ×0.2. On all other occasions, the diesel generator ran for the same amount

of time despite the additional available wind energy (higher multiplication factor). However, more energy was being dissipated in the 5 kW secondary loads as it got windier throughout the day in order to avoid the batteries being charged to 100%. From Fig. 24, it can be observed that the SOC deviated from the ideal case (×1) quite significantly even with just a small difference in wind speed. Comparing the load sensitivity and the wind speed sensitivity SOC results (Fig. 23 and Fig. 24), it can be concluded that the battery SOC is more sensitive to the wind speed forecast error than the load forecast error. Thus, it is important to emphasise that an accurate wind speed forecast is vital in order for the proposed optimise operation to work satisfactory.

Wind speed multiplication factor	*×0.8*	*×1*	*×1.2*	*×1.4*
Average frequency (Hertz)	50.00	50.01	50.01	50.02
Average line-to-line voltage (Volt)	396.06	395.75	395.28	394.78
Diesel generator turn-on time (minutes)	219.80	79.69	79.70	79.71
3 kW secondary load turn-on time (minutes)	0	54.08	298.32	438.69
5 kW secondary load turn-on time (minutes)	0	0	123.92	278.25

Table 4: Wind speed sensitivity simulation results

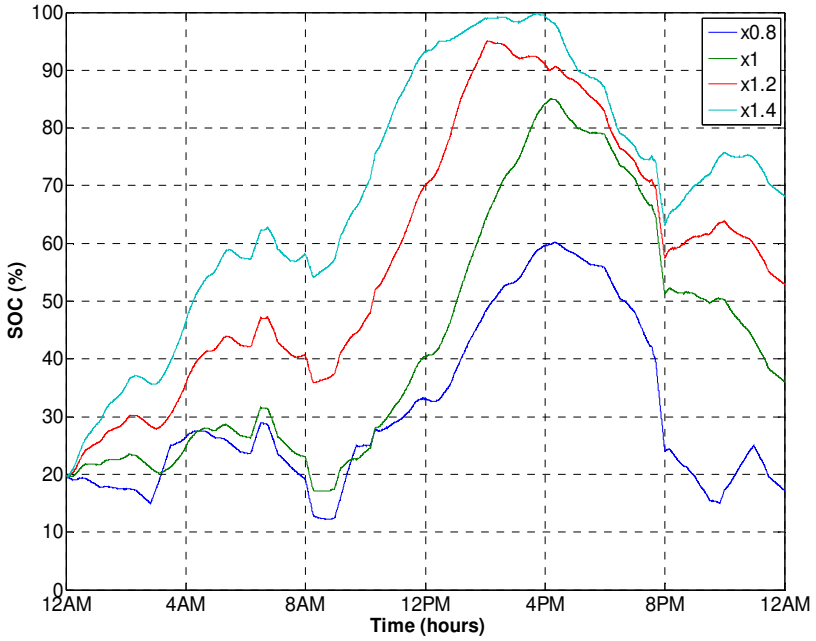

Fig. 24: SOC profiles for different wind speed multiplication factors

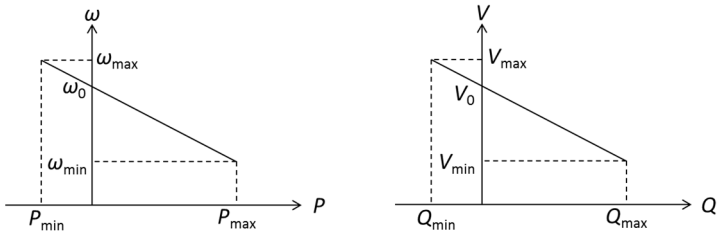

Fig. 25: P-ω and Q-V droop characteristics

4.3 Time-shifted Load Sensitivity Analysis

A random time-shifting approach of aggregating the three households was implemented for the second phase of load sensitivity analysis. As shown in Fig. 26, the load profile for the second household was obtained by delaying the load profile from the first household with a random number. The random number generator produced a random number which was set to have a mean value of 30 and variance of 20. Therefore, the load profile would be randomly time-shifted, however the mean delay time was set at 30 minutes. The mean value of the random number generator of the third household was 60 and variance of 20. On average, the third household load profile had a delay of one hour relative to the first household load profile. Finally, a summation was performed on the three households, producing a load profile as portrayed in Fig. 27. Note that the morning and evening peaks did not occur at the exact same time and therefore, it is expected that the discharging rate of the batteries during this period should be lower.

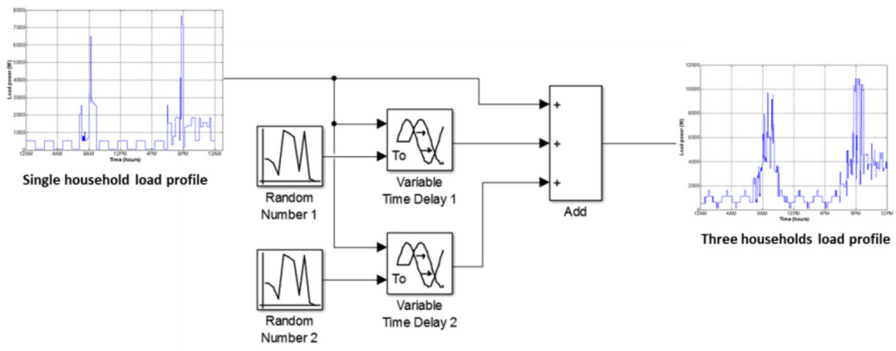

Fig. 26: Simulink implementation of load aggregation model with random number generators

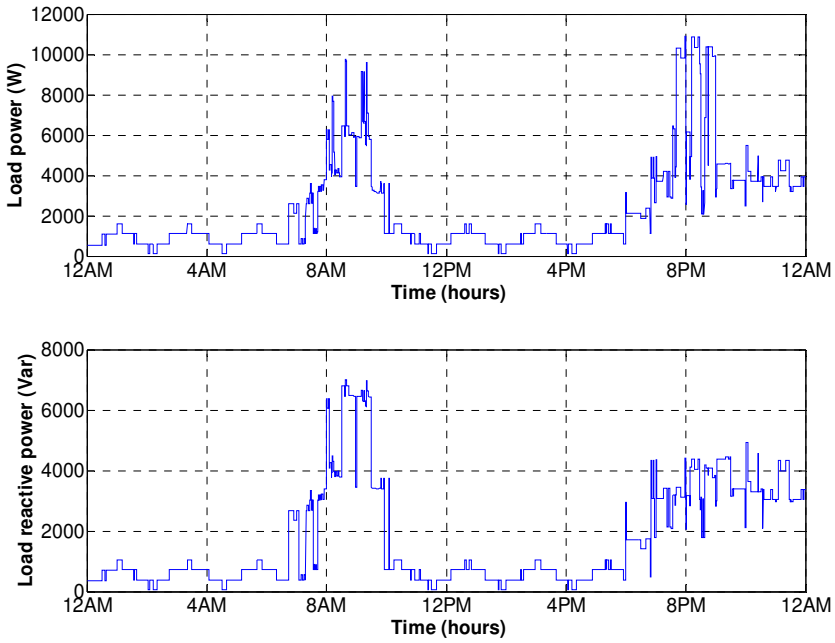

Fig. 27: Load profile for three households (time-shifted for second and third household)

Using the above-mentioned load profile, a sensitivity analysis was carried out. Multiplication factors of ×0.8, ×1, ×1.2 and ×1.4 were applied to the new load profile in Fig. 27 with 24 hours of simulation performed for each scenario. Table 5 and Fig. 28 show the simulation results and SOC profiles for all scenarios, respectively. The average frequency and average voltage show that the hybrid system operated in a stable manner. The diesel generator's running time for the case of ×1.2 and ×1.4 tabulated in Table 5 is observed to be less than that in Table 3. This was due to the morning peak magnitude in new load profile being significantly less than the previous case which reduced the discharging rate of the batteries. In addition, it decreased the risk of having the SOC fall below the pre-set safety threshold level. In addition, it was apparent that the discharging rate of the batteries for the evening peak load at 8pm was smaller for the case in Fig. 28 than the results shown in Fig. 23. Overall, the SOCs for both studies are similar despite the differences between the load profile patterns. With this study, the robustness of the proposed hybrid system optimised operation was being tested.

Wind speed multiplication factor	*×0.8*	*×1*	*×1.2*	*×1.4*
Average frequency (Hertz)	50.01	50.01	50.01	50.01
Average line-to-line voltage (Volt)	396.19	395.77	395.34	394.97
Diesel generator turn-on time (minutes)	79.70	79.70	79.70	151.07
3 kW secondary load turn-on time (minutes)	166.75	69.83	0	0
5 kW secondary load turn-on time (minutes)	0	0	0	0

Table 5: Time-shifted load sensitivity simulation results

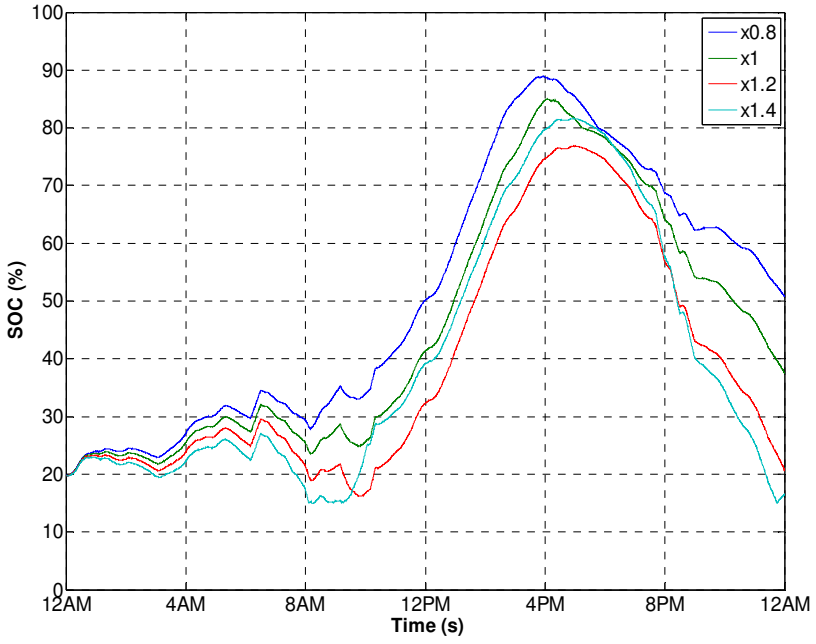

Fig. 28: SOC profiles for different time-shifted load multiplication factors

5. Conclusion

In conclusion, the proposed optimisation algorithm to optimise the operation of a hybrid wind-diesel-battery system has been thoroughly tested with various scenarios and its robustness is proven. A slightly different approach was taken in this work where the diesel generator operation was optimised by having a controlled number of start-stop cycles in addition to a fixed power output whenever it was switched-on. This proposed control algorithm required the forecasted wind speed and the load demand to be part of the input data, besides defining the constraints during the optimisation process. As pointed out earlier, some safety pre-cautions are needed to ensure the hybrid system operates in a stable manner during any unexpected events. In order to simulate a more realistic scenario, measured wind speed was utilised. For the load profile, a three household bottom-up load model was adopted. The optimised results generated mathematically were post-processed and verified using the hybrid system which was developed from Simulink's SimPowerSystems. Through this, the contrast in results between the simple mathematical modelling and the physical modelling were clearly demonstrated. It was shown that there were discrepancies between the two and it has proven the importance of the latter. The physical models built from the SimPowerSystems contain the electrical and mechanical information, whereas simple mathematical models only descript the system operation through arithmetic operations. This technique allows the hybrid system designers to investigate the factors which contribute to the non-ideal behaviours of the hybrid system in the real world. Therefore, more confidence can be gained by verifying the mathematical modelling using the physical models. However, the physical simulation demands a large computation effort and therefore it incurs much longer simulation time. Ultimately, it was shown that the diesel generator was able to operate in a stable manner in the off-grid scenario, with a fixed power output whenever it was switched-on. It is believed that such optimised operation can pro-long the lifetime of the diesel generator significantly.

6. Acknowledgement

The work is supported by Gaia Wind Ltd., Commonwealth Scholarship Commission and The University of Edinburgh.

7. References

[1] M. S. Ismail, M. Moghavvemi, and T. M. I. Mahlia, "Techno-economic analysis of an optimized photovoltaic and diesel generator hybrid power system for remote houses in a tropical climate," *Energy Conversion and Management,* vol. 69, pp. 163-173, 2013.

[2] M. Bortolini, M. Gamberi, A. Graziani, and F. Pilati, "Economic and environmental bi-objective design of an off-grid photovoltaic–battery–diesel generator hybrid energy system," *Energy Conversion and Management,* vol. 106, pp. 1024-1038, 2015.

[3] D. Tsuanyo, Y. Azoumah, D. Aussel, and P. Neveu, "Modeling and optimization of batteryless hybrid PV (photovoltaic)/Diesel systems for off-grid applications," *Energy,* vol. 86, pp. 152-163, 2015.
[4] J. K. Kaldellis, *Stand-Alone and Hybrid Wind Energy Systems: Technology, Energy Storage and Applications*: Woodhead Publishing Ltd, 2010.
[5] D. Das, S. K. Aditya, and D. P. Kothari, "Dynamics of diesel and wind turbine generators on an isolated power system," *International Journal of Electrical Power & Energy Systems,* vol. 21, pp. 183-189, 1999.
[6] P. A. Stott, "Renewable Variable Speed Hybrid System," PhD Thesis, The University of Edinburgh, Edinburgh, 2010.
[7] H. Tazvinga, B. Zhu, and X. Xia, "Energy dispatch strategy for a photovoltaic–wind–diesel–battery hybrid power system," *Solar Energy,* vol. 108, pp. 412-420, 2014.
[8] B. Zhu, H. Tazvinga, and X. Xia, "Model Predictive Control for Energy Dispatch of a Photovoltaic-Diesel-Battery Hybrid Power System," *IFAC Proceedings Volumes,* vol. 47, pp. 11135-11140, 2014.
[9] M. A. Elhadidy and S. M. Shaahid, "Decentralized/stand-alone hybrid Wind–Diesel power systems to meet residential loads of hot coastal regions," *Energy Conversion and Management,* vol. 46, pp. 2501-2513, 2005.
[10] Y. Hu, J. M. Morales, S. Pineda, M. J. Sánchez, and P. Solana, "Dynamic multi-stage dispatch of isolated wind–diesel power systems," *Energy Conversion and Management,* vol. 103, pp. 605-615, 2015.
[11] C. Dennis Barley and C. Byron Winn, "Optimal dispatch strategy in remote hybrid power systems," *Solar Energy,* vol. 58, pp. 165-179, 1996.
[12] X. Wang, A. Palazoglu, and N. H. El-Farra, "Operational optimization and demand response of hybrid renewable energy systems," *Applied Energy,* vol. 143, pp. 324-335, 2015.
[13] M. S. Ismail, M. Moghavvemi, and T. M. I. Mahlia, "Genetic algorithm based optimization on modeling and design of hybrid renewable energy systems," *Energy Conversion and Management,* vol. 85, pp. 120-130, 2014.
[14] J. Zeng, M. Li, J. F. Liu, J. Wu, and H. W. Ngan, "Operational optimization of a stand-alone hybrid renewable energy generation system based on an improved genetic algorithm," in *IEEE Power and Energy Society General Meeting*, 2010, pp. 1-6.
[15] H. Dagdougui, R. Minciardi, A. Ouammi, M. Robba, and R. Sacile, "A dynamic decision model for the real-time control of hybrid renewable energy production systems," *IEEE Systems Journal,* vol. 4, pp. 323-333, 2010.
[16] D. Cormode, A. D. Cronin, W. Richardson, A. T. Lorenzo, A. E. Brooks, and D. N. DellaGiustina, "Comparing ramp rates from large and small PV systems, and selection of batteries for ramp rate control," in *39th Photovoltaic Specialists Conference (PVSC)*, 2013, pp. 1805-1810.
[17] A. Mohammed, J. Pasupuleti, T. Khatib, and W. Elmenreich, "A review of process and operational system control of hybrid photovoltaic/diesel generator systems," *Renewable and Sustainable Energy Reviews,* vol. 44, pp. 436-446, 2015.
[18] M. Q. Raza and A. Khosravi, "A review on artificial intelligence based load demand forecasting techniques for smart grid and buildings," *Renewable and Sustainable Energy Reviews,* vol. 50, pp. 1352-1372, 2015.
[19] S. Hassan, A. Khosravi, J. Jaafar, and M. A. Khanesar, "A systematic design of interval type-2 fuzzy logic system using extreme learning machine for electricity load demand forecasting," *International Journal of Electrical Power & Energy Systems,* vol. 82, pp. 1-10, 2016.
[20] M. Yesilbudak, S. Sagiroglu, and I. Colak, "A new approach to very short term wind speed prediction using k-nearest neighbor classification," *Energy Conversion and Management,* vol. 69, pp. 77-86, 2013.
[21] I. Colak, S. Sagiroglu, M. Yesilbudak, E. Kabalci, and H. I. Bulbul, "Multi-time series and -time scale modeling for wind speed and wind power forecasting part II: Medium-term and long-term applications," in *International Conference on Renewable Energy Research and Applications (ICRERA)*, 2015, pp. 215-220.
[22] A. Messac, *Optimization in Practice with MATLAB®: For Engineering Students and Professionals*: Cambridge University Press, 2015.
[23] D. A. Coley, *An Introduction to Genetic Algorithms for Scientists and Engineers*: World Scientific, 1999.
[24] J. Arora, *Introduction to Optimum Design*, 3rd ed.: Academic Press, 2011.
[25] P. Venkataraman, *Applied Optimization with MATLAB Programming*, 2nd ed.: John Wiley & Sons, 2009.
[26] "Sunny Island 8.0H / 6.0H installation manual," *SMA*.

[27] M. Braun, "Models for Transient Simulations of Decentral Power Generation - Implementation and Verification in PowerFactory," Universität Stuttgart & Institut für Solare Energieversorgungstechnik (ISET), Stuttgart, Germany, 2005.
[28] S. M. Cuk, "Modelling, Analysis and Design of Switching Converters," PhD thesis, California Institute of Technology Pasadena, California, 1977.
[29] L. K. Gan, D. E. Macpherson, and J. K. H. Shek, "Synchronisation control and operation of microgrids for rural/island applications," in *48th International Universities' Power Engineering Conference (UPEC)*, 2013.
[30] L. K. Gan, J. K. H. Shek, and M. A. Mueller, "Modelling and experimentation of grid-forming inverters for standalone hybrid wind-battery systems," in *2015 4th International Conference on Renewable Energy Research and Applications (ICRERA)*, Palermo, Italy, 2015.
[31] P. Jain, *Wind Energy Engineering*: McGraw-Hill Professional, 2010.
[32] "Power Performance Certification Test of a Model GW 133-11 Wind Turbine," *TUV NEL Ltd., Report No. 2010/204,* , 2010.
[33] "Design Aeroelastic Loads Gaia-Wind 11kW Turbine 18[m] Tubular Tower," *Gaia Wind Ltd., Report No. GWTD0028,* , 2011.
[34] S. Krishnamurthy, T. M. Jahns, and R. H. Lasseter, "The operation of diesel gensets in a CERTS microgrid," in *IEEE Power and Energy Society General Meeting - Conversion and Delivery of Electrical Energy in the 21st Century*, 2008, pp. 1-8.
[35] S. D. Alley, "Generator Basics: Applied to Field Problems," *ANNA Inc.*, 1993.
[36] M. J. Hu and G. F. Yang, "Simulation of Speed Controlling System on Diesel Engine Based on FN," in *Fourth International Symposium on Knowledge Acquisition and Modeling (KAM)*, 2011, pp. 358-361.
[37] J. Mamboundou and N. Langlois, "Application of indirect adaptive model predictive control supervised by fuzzy logic to a diesel generator," in *9th IEEE International Conference on Control and Automation (ICCA)*, 2011, pp. 1037-1043.
[38] C. Mai, K. Jepsen, Y. Zhenyu, L. Hansen, and K. K. Madsen, "Intelligent control of diesel generators using gain-scheduling: Based on online external-load estimation," in *International Electronics and Application Conference and Exposition (PEAC)*, 2014, pp. 966-971.
[39] K. E. Yeager and J. R. Willis, "Modeling of emergency diesel generators in an 800 megawatt nuclear power plant," *IEEE Transactions on Energy Conversion,* vol. 8, pp. 433-441, 1993.
[40] A. Capasso, W. Grattieri, R. Lamedica, and A. Prudenzi, "A bottom-up approach to residential load modeling," *IEEE Transactions on Power Systems,* vol. 9, pp. 957-964, 1994.
[41] I. Richardson, M. Thomson, D. Infield, and C. Clifford, "Domestic electricity use: A high-resolution energy demand model," *Energy and Buildings,* vol. 42, pp. 1878-1887, 2010.
[42] R. Yao and K. Steemers, "A method of formulating energy load profile for domestic buildings in the UK," *Energy and Buildings,* vol. 37, pp. 663-671, 2005.
[43] L. K. Gan, J. K. H. Shek, and M. A. Mueller, "Hybrid wind–photovoltaic–diesel–battery system sizing tool development using empirical approach, life-cycle cost and performance analysis: A case study in Scotland," *Energy Conversion and Management,* vol. 106, pp. 479-494, 2015.
[44] C. Nichita, D. Luca, B. Dakyo, and E. Ceanga, "Large band simulation of the wind speed for real time wind turbine simulators," *IEEE Transactions on Energy Conversion,* vol. 17, pp. 523-529, 2002.
[45] N. Stannard and J. R. Bumby, "Performance aspects of mains connected small-scale wind turbines," *IET Generation, Transmission & Distribution,* vol. 1, pp. 348-356, 2007.
[46] C. Anderson, "Chapter 3: Wind Turbine Aerodynamics," *University of Edinburgh, Principles of Wind Energy Lecture Notes 2012*.
[47] B.-M. Hodge, A. Florita, K. Orwig, D. Lew, and M. Milligan, "A Comparison of Wind Power and Load Forecasting Error Distributions," presented at the 2012 World Renewable Energy Forum Denver, Colorado, 2012.
[48] B.-M. Hodge and M. Milligan, "Wind Power Forecasting Error Distributions over Multiple Timescales," presented at the Power & Energy Society General Meeting, Michigan, 2011.
[49] M. Brower, "Wind Energy Forecasting," ed. Cambridge, United States: Massachusetts Institute of Technology (MIT), 2011.